NAVAL POSTGRADUATE SCHOOL

MONTEREY, CALIFORNIA

THESIS

DETECTION AND RESOLVABILITY OF PULSED ACOUSTIC SIGNALS THROUGH THE SOUTH CHINA SEA BASIN: A MODELING ANALYSIS

by

Adria R. Schneck-Scott

September 2005

Thesis Advisor:	Ching-Sang Chiu
Co-Advisors:	Chris Miller
	John Joseph

Approved for public release; distribution is unlimited

THIS PAGE INTENTIONALLY LEFT BLANK

REPORT DOCUMENTATION PAGE			Form Approved OMB No. 0704-0188
Public reporting burden for this collection of information is estimated to average 1 hour per response, including the time for reviewing instruction, searching existing data sources, gathering and maintaining the data needed, and completing and reviewing the collection of information. Send comments regarding this burden estimate or any other aspect of this collection of information, including suggestions for reducing this burden, to Washington headquarters Services, Directorate for Information Operations and Reports, 1215 Jefferson Davis Highway, Suite 1204, Arlington, VA 22202-4302, and to the Office of Management and Budget, Paperwork Reduction Project (0704-0188) Washington DC 20503.			
1. AGENCY USE ONLY ***(Leave blank)***	**2. REPORT DATE** September 2005	**3. REPORT TYPE AND DATES COVERED** Master's Thesis	
4. TITLE AND SUBTITLE: Detection and Resolvability of Pulsed Acoustic Signals Through the South China Sea Basin: A Modeling Analysis			**5. FUNDING NUMBERS**
6. AUTHOR(S) Adria R Schneck-Scott			
7. PERFORMING ORGANIZATION NAME(S) AND ADDRESS(ES) Naval Postgraduate School Monterey, CA 93943-5000			**8. PERFORMING ORGANIZATION REPORT NUMBER**
9. SPONSORING /MONITORING AGENCY NAME(S) AND ADDRESS(ES) N/A			**10. SPONSORING/MONITORING AGENCY REPORT NUMBER**
11. SUPPLEMENTARY NOTES The views expressed in this thesis are those of the author and do not reflect the official policy or position of the Department of Defense or the U.S. Government.			
12a. DISTRIBUTION / AVAILABILITY STATEMENT Approved for public release; distribution is unlimited			**12b. DISTRIBUTION CODE**

13. ABSTRACT (maximum 200 words)

Sponsored by the office of Naval Research (ONR), the Windy Islands Soliton Experiment (WISE) is designed to measure acoustic propagation and physical oceanography commencing April 2005-2006. As part of this experiment, two deep water moorings with acoustic transceivers (source-receiver combinations) will be placed in the South China Sea deep basin 160 km apart. These transceivers will transmit and receive phase-modulated signals (pulses after signal processing) over the year attempting to (1) capture multi-scale variability in transmission loss and (2) examine the progression of internal tides within the basin through tomographic inverse techniques. Acoustic arrival structure modeling was conducted to discern whether a detectable and resolvable signal was to be expected and for signal design. Using a stochastic inverse approach, the inversion was used to determine vertical structure, spatial resolution, and uncertainty associated with the tomographic mapping of the internal tide.

14. SUBJECT TERMS soliton, oceanography, internal tide, acoustic propagation, ray theory, pulsed acoustic signals, South China Sea, acoustic detection, modeling analysis			**15. NUMBER OF PAGES** 45
			16. PRICE CODE
17. SECURITY CLASSIFICATION OF REPORT Unclassified	**18. SECURITY CLASSIFICATION OF THIS PAGE** Unclassified	**19. SECURITY CLASSIFICATION OF ABSTRACT** Unclassified	**20. LIMITATION OF ABSTRACT** UL

NSN 7540-01-280-5500 Standard Form 298 (Rev. 2-89)
Prescribed by ANSI Std. 239-18

THIS PAGE INTENTIONALLY LEFT BLANK

Approved for public release; distribution is unlimited

DETECTION AND RESOLVABILITY OF PULSED ACOUSTIC SIGNALS THROUGH THE SOUTH CHINA SEA BASIN: A MODELING ANALYSIS

Adria R Schneck-Scott
Lieutenant, United States Navy
B.S., United States Naval Academy, 1997

Submitted in partial fulfillment of the requirements for the degree of

MASTER OF SCIENCE IN PHYSCIAL OCEANOGRAPHY

from the

NAVAL POSTGRADUATE SCHOOL
September 2005

Author:

Adria R Schneck-Scott

Approved by:

Ching-Sang Chiu
Thesis Advisor

Chris Miller
Co-Advisor

John Joseph
Co-Advisor

Mary L Batteen
Chairman Department of Oceanography

THIS PAGE INTENTIONALLY LEFT BLANK

ABSTRACT

Sponsored by the office of Naval Research (ONR), the Windy Islands Soliton Experiment (WISE) is designed to measure acoustic propagation and physical oceanography commencing April 2005-2006. As part of this experiment, two deep water moorings with acoustic transceivers (source-receiver combinations) will be placed in the South China Sea deep basin 160 km apart. These transceivers will transmit and receive phase-modulated signals (pulses after signal processing) over the year attempting to (1) capture multi-scale variability in transmission loss and (2) examine the progression of internal tides within the basin through tomographic inverse techniques. Acoustic arrival structure modeling was conducted to discern whether a detectable and resolvable signal was to be expected and for signal design. Using a stochastic inverse approach, the inversion was used to determine vertical structure, spatial resolution, and uncertainty associated with the tomographic mapping of the internal tide.

THIS PAGE INTENTIONALLY LEFT BLANK

TABLE OF CONTENTS

THIS PAGE INTENTIONALLY LEFT BLANK

LIST OF FIGURES

THIS PAGE INTENTIONALLY LEFT BLANK

LIST OF TABLES

THIS PAGE INTENTIONALLY LEFT BLANK

ACKNOWLEDGMENTS

First and foremost, I would like to thank Professor Ching-Sang Chiu, my thesis advisor. Your guidance, patience, and flexibility opened a world of knowledge and interest not limited to this study. I am very honored to be your last masters' student and appreciate all you have given.

If it were not for the mass assistance of Chris Miller, I would still be working this thesis. Many thanks for this and your friendship throughout this study.

Additional thanks goes to CDR John Joseph. Your professional guidance and confidence allowed me to accomplish more than this thesis. I hope my appreciation is clearly understood.

Lastly, but certainly not least, I would like to thank my husband and children. Certainly I would not be where I am today if it were not for your love and support. You are my darlings and my passion. I am truly grateful and blessed by you each and every day.

THIS PAGE INTENTIONALLY LEFT BLANK

I. INTRODUCTION

A. SOUTH CHINA SEA BACKGROUND

The westernmost of several marginal seas in the western Pacific Ocean, the South China Sea stretches from Singapore to Taiwan bordered by the Straits of Malacca to the south, Luzon Strait to the east, and Taiwan Strait to the northeast. The bottom consists of two extended continental shelves, north and south, and a deep basin with max depth of 5000 m in the central eastern side. The climate is one of tropical monsoon.

The South China Sea is home to several interesting oceanographic features including large amplitude internal waves. Isolated packets of large amplitude, nonlinear internal waves are often described as solitons (Ramp, et al., 2004). The largest ever observed internal waves occur in this region (Hsu, Liu, 2000). Although the generation area is still debated, it is generally assumed that these large amplitude internal waves are generated by tidal flow across large topographic features such as the shallow ridges in the Luzon Strait. These generation mechanisms, including the influences of the tide and Kuroshio intrusion into the South China Sea and their evolution across the deep basin are still under investigation, however they appear to be linked to the internal tide. No measurements of internal wave generation or tidal transbasin transit exist. Figure 1 is a composite sketch of the internal wave distribution developed by Hsu and Liu (2000) compiled from hundreds of Synthetic Aperture Radar (SAR) images from the First European Remote Sensing Satellite (ERS-1) images during 1993-1999. It is evident from this figure that internal waves are not detected by satellite remote sensing as they transit the deep basin. Due to spatial changes in stratification, they could be divided into deeper depths (Chiu, 2004). This study investigates whether tomography can be used to study the internal tides as they transit the deep basin in hopes it can lead to better understanding of the internal wave phenomenon.

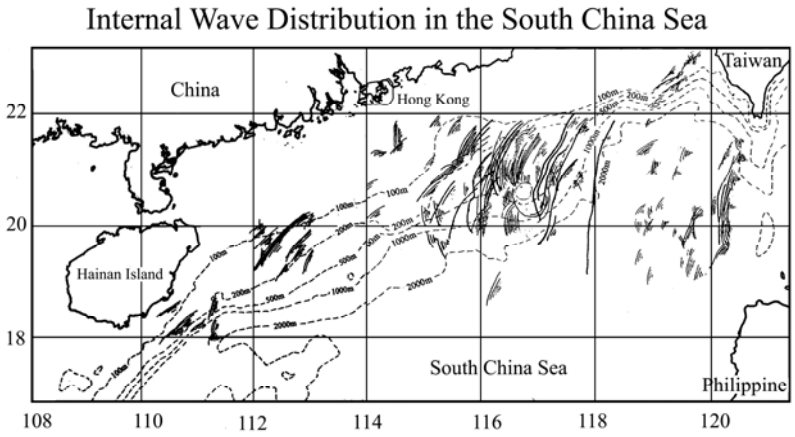

Figure 1. Composite sketch of internal waves in South China Sea based on SAR images courtesy of Hsu and Liu (2000).

B. STRATEGIC IMPORTANCE

The South China Sea is rich in resources, especially oil and gas. Overlapping claims of sovereignty over the many mid-ocean islands, other land features and surrounding waters cause risk of military confrontation among the claimants (Hull, 1996). Some nations have been reluctant to discuss sovereignty issues multilaterally, which worries other nations in the region. Although sovereignty claims are regional issues that can only be solved by the claimants, the United States is viewed by the region as the major military deterrent to any nation's forceful sovereignty and has vital interest in keeping the South China Sea open to ships of all nations (Hull, 1996).

In *Sea Power 21*, Admiral Vern Clark states information superiority and knowledge dominance leads to unprecedented offensive power, defensive assurance, and operational independence to today's warfighters. Accurate battlespace characterization and precise knowledge of the environment help create this advantage. Understanding and predicting the generation and evolution of these highly nonlinear internal waves linked to the internal tide and their impact on the acoustic environment can provide strategic and tactical advantage over adversaries operating in this area. The Asian Seas International Acoustic Experiment (ASIAEX) conducted in spring of 2001 measured solitons on the Chinese continental shelf. Temperature variations resulting from this phenomenon measured greater than 9^{o} C at 130 m (Ramp et al., 2004). This rapid temperature change can have serious impacts on naval operations in the region. Thus, as Naval Officers, and

especially Naval Oceanographers, it is of utmost importance to understand the unique oceanography observed in the South China Sea and eventually predict it for avoidance and/or tactical advantage. This investigation and WISE are helping to accomplish this understanding.

C. WINDY ISLANDS SOLITON EXPERIMENT (WISE)

WISE is a collaborative acoustics and physical oceanography experiment between National Taiwan University, National Sun Yet-Sen University, Ocean Acoustical Services and Instrumentation Systems (OASIS), Woods Hole Oceanographic Institute, and Naval Postgraduate School (NPS). The experiment will last for one year, April 2005-2006, and take place in the South China Sea and Luzon Strait.

The acoustic portion of the experiment will take place in two parts. One, the shelf component which is not discussed in this thesis; the other the basin component, whose objective is to study and characterize the impacts of transbasin, nonlinear waves on long-range transmission loss, and monitor the evolution of transbasin internal tides within the basin. This portion of the experiment will consist of two transceivers (source-receiver combinations) on deep moorings B1 and B2 whose positions are shown in Figure 2. These transceivers will be moored at 800 m and transmit and receive reciprocal phase-modulated signals for one year starting in April 2005. The range will be approximately 160 km and transducers have been designed to transmit a 25.5 s signal, which corresponds to a 10 ms pulse after pulse-compression signal processing, every ten minutes.

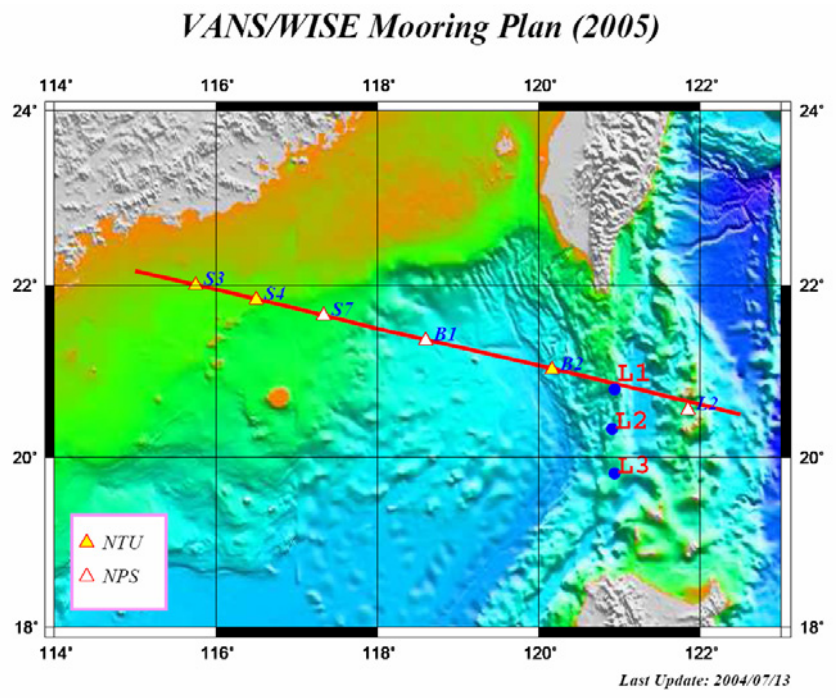

Figure 2. Proposed mooring locations for WISE. S3, S4, and S7 are shallow water moorings. L1 through 3 are Luzon Strait moorings. B1 and B2 are deep basin moorings. Acoustic transceivers on B1 and B2 will be placed at 800 m depth, 160 km apart. Figure is courtesy of Chiu, 2004.

D. OCEAN ACOUSTIC TOMOGRAPHY

Ocean acoustic tomography uses data of long-range acoustic propagation to obtain information about the ocean interior. It is a tool with which we can infer and study the state of the ocean traversed by a sound field using precise measurements of travel time or other acoustic propagation properties. It takes advantage of the fact that acoustic propagation properties, like travel time, are a function of sound speed, which is a function of temperature. There are many advantages of ocean tomography over other ocean sampling methods. Because the ocean is nearly transparent to low-frequency sound, it can be transmitted thousands of kilometers. Traditional method of collecting data via research vessels and construction of synoptic fields is time-consuming and costly. At approximately 1500 m/s, sound travels fast, allowing acoustic tomography the ease of areal coverage. Since relatively few acoustic moorings are required for ocean tomography, it is cheaper and offers many more distinct ray paths than traditional

observational mooring systems. Also, it permits observation of areas that are challenging to observe directly. For these reasons, ocean acoustic tomography is of considerable interest in oceanography. (Munk, et al., 1995)

Ocean acoustic tomography is a two-part problem consisting of the forward and inverse problem. The inverse method of tomography first demands solving and understanding the forward problem. The forward problem is the classical problem of finding a solution to the wave equation for sound propagation through a modeled ocean region. The inverse problem demands calculation of ocean properties given properties of the transmitted and received signals. The tomography used in this study compares the measured arrival pattern to a modeled arrival pattern computed for a climatologically mean ocean. If a signal arrives earlier than predicted, this would indicate in-situ temperatures are above the climatological mean and vice versa. Differences between the observed and modeled arrival structures contain oceanographic information about the entire sound speed field. Exploiting this information is what the inverse method seeks to do. (Munk, et al., 1995)

Inversions require arrivals to be resolvable, identifiable, stable, and have adequate signal-to-noise ratios (SNR). Applicability of acoustic tomography is dependant on these things. Resolvability requires arrival time separation between eigenrays to be adequate to distinguish individual rays. Identifiably requires each eigenray arrival time to closely match that of the modeled arrival time allowing recognition of individual raypaths. Stability requires the same arrival structure and eigenrays to exist over successive transmissions without fading or disappearing. Adequate SNR is required to ensure our arrivals are strong enough to be heard over background noise and to ensure precise travel times.

E. THESIS OBJECTIVE AND APPROACH

There are three principle objectives of this thesis. The first is to investigate the detectability of multi-path arrivals. The second objective is to investigate the resolvability of individual ray arrivals. The third objective seeks to answer the scientific question of whether tomography can be used to observe and monitor the internal tide as it transits the deep basin. The first two objectives were achieved by modeling the multi-path arrival

structure using ray theory. Modeling was used to investigate whether strong, resolvable arrivals exist. Competing bottom characteristic hypotheses were examined as was signal processing gain. The goal was to maximize the number of detectable and resolvable signals to gain adequate SNR and improve tomographic resolution.

Briefly, the analysis involved two steps. First, acoustic propagation modeling was accomplished to predict the expected ray arrival structure. This was achieved by first defining the environment. A reference or "background" sound speed profile obtained from the Naval Oceanographic Office (NAVO) Generalized Digital Environmental Model (GDEM) and high resolution data obtained from the NAVO bathymetry database, DBDV-V, were used as the model ocean. Competing bottom characteristics hypotheses were used to measure expectant SNRs for both best and worst case scenarios and post experiment remedies if necessary. Sea state information was gathered from National Oceanic and Atmospheric Administration (NOAA) climatological database. Multi-path arrival synthesis was then accomplished using ray theory.

Secondly, a resolution and variance analysis was conducted. The horizontal resolution along the acoustic path was estimated by constraining the vertical structure. Vertical structure was constrained by dynamical sound speed perturbation modes derived using the NAVO GDEM data.

F. THESIS OUTLINE

The remainder of this thesis consists of three chapters. Chapter II presents and discusses propagation modeling results. Chapter III presents the internal tide vertical structure calculation, a discussion of the horizontal resolution of the tomographic estimate, and discussion of the practicality of using tomography to monitor internal tides. Conclusions are given in Chapter IV.

II. PROPAGATION MODELING

A. EXPERIMENTAL DESIGN

Propagation model inputs were based on the WISE design. WISE hopes to use ocean acoustic tomography to study transbasin internal tides and their effect on the internal wave phenomenon. Ocean acoustic tomography requires accurately measured travel times. Acquiring accurate travel time data demands using broadband coded source signals with accurate synchronization of transmissions and recordings. Pulse-compression techniques are needed to gain adequate SNRs from power limited sources without degrading the resolution of the signal (Munk, et al., 1995). WISE deep basin moorings will be positioned at 800 m depth, 160 km apart. The sound source used during this experiment will operate at a centerline frequency of 400 Hz, which has 100 Hz bandwidth and will transmit a 5.11 second, 511 digit pseudo-random (m-sequence) at 180 dB/1 μPa at 1 m. This corresponds to a 10 ms pulse after pulse compression and signal processing. The receiver system was built to resolve the positive and negative arrival differences. The phase modulation angle is 87.46035^{o}. During reception, data is demodulated and coherently averaged. Expectant processing gains of 33 dB are shown in Table 1. Each mooring will also sample current, temperature, and salinity using a variety of sensors. In order to resolve the internal wave field, these instruments must sample rapidly (order 2 minutes). Battery and memory constraints dictate the instruments be serviced every 3 months for the entire 1 year experiment. Additionally, the transmission source will be turned off when not in use.

The in-band ambient noise estimate is based on Wentz curves and NOAA climatological data. These data indicate a monthly mean of at least sea state 3 for this portion of the South China Sea, with the exception of May. A noise level of 68 dB results from Sea state 3, at 400 Hz. Additional noise over the bandwidth is 20 dB. The resulting ambient noise calculation is 88 dB re 1 μPa. Similar calculations for sea state 1 result in 77 dB re 1 μPa.

Table 1. Processing gains expected for deep basin receivers.

Coherent Averaging	10 log(4) = 6 dB
Pulse Compression	10 log(511) = 27 dB

B. HAMILTON RAY TRACING

The tomographic inverse solution cannot be completed without first solving the forward problem. This can be achieved using ray theory. Ray theory surmises a received signal is the summation of many different arrivals, each traveling along a distinct path between the source and receiver called an eigenray. Receiver pressure disturbances are associated with the eigenrays, each having their own time delays, amplitudes, and phase shifts. Mathematically, the received signal is expressed as:

$$\tilde{r}(t)=\Sigma a_n \tilde{s}(t-t_n)e^{-i(2\pi f_o t_n+\phi_n)}$$

where $\tilde{r}(t)$ is the received signal's complex envelope, $\tilde{s}(t)$ is the emitted signal's complex envelope, f_o is the transmission carrier frequency, and t_n, a_n, and φ_n are the eigenray's time delay, amplitude modification, and phase shift, respectively. Therefore, modeling arrival structure requires ray tracing and determination of delay, magnitude, and phase parameters.

Ray paths were calculated using the upgraded (Chiu, et al., 1994) three-dimensional ray-tracing program HARPO, Hamiltonian Acoustic Raytracing Program for the Ocean (Jones et al., 1986). HARPO traces rays by numerically integrating Hamilton's equations of motion in spherical coordinates with a set of initial conditions. A model ocean, which consists of a continuous representation of the sound speed field and two-dimensional representation of the upper and lower reflecting surfaces, is required by HARPO. The upper reflecting surface is the ocean surface, the lower the ocean bottom. This continuous representation of sound speed and bathymetry eliminates problems of false caustics and discontinuous raypath properties (Jones et al., 1986). Historical sound speed and bathymetry data compiled from NAVO database were filtered using Butterworth filters. This was done to smooth the data, preventing unreal ray chaos. Figures 3(a) and 3(b) show the mean sound speed profile and bathymetry used in HARPO.

Ray launch angles from -30^o to +30^o at an increment of .005^o, were also inputted into HARPO. Rays with launch angles greater than +15^o and less than -15^o suffered numerous bottom interactions. This resulted in high cumulative bottom loss. Hence, the rays outside this envelope were not included in further analyses. Figure 4 shows the geometry of the eigenray paths.

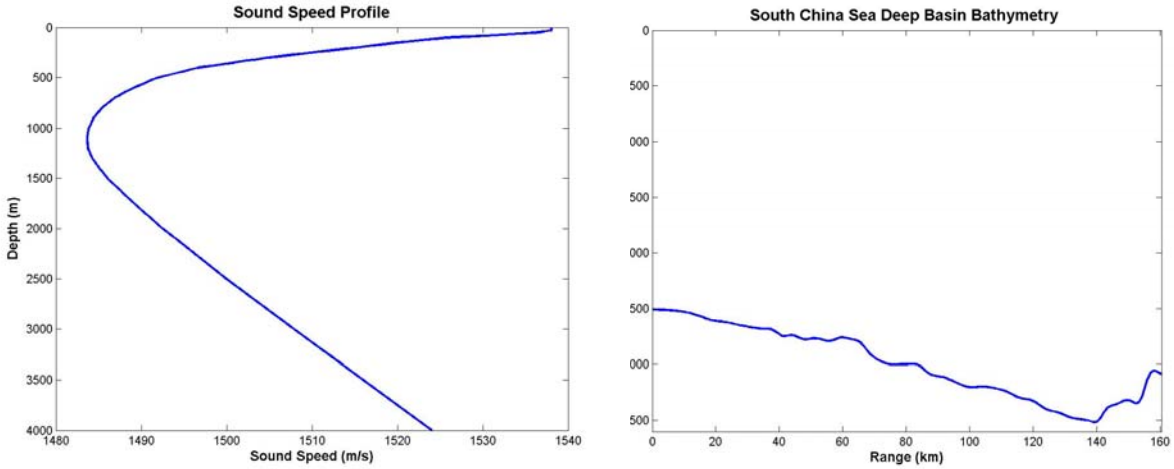

Figure 3. (a) and (b). Smoothed South China Sea sound speed field (a) and bathymetry (b) used in HARPO.

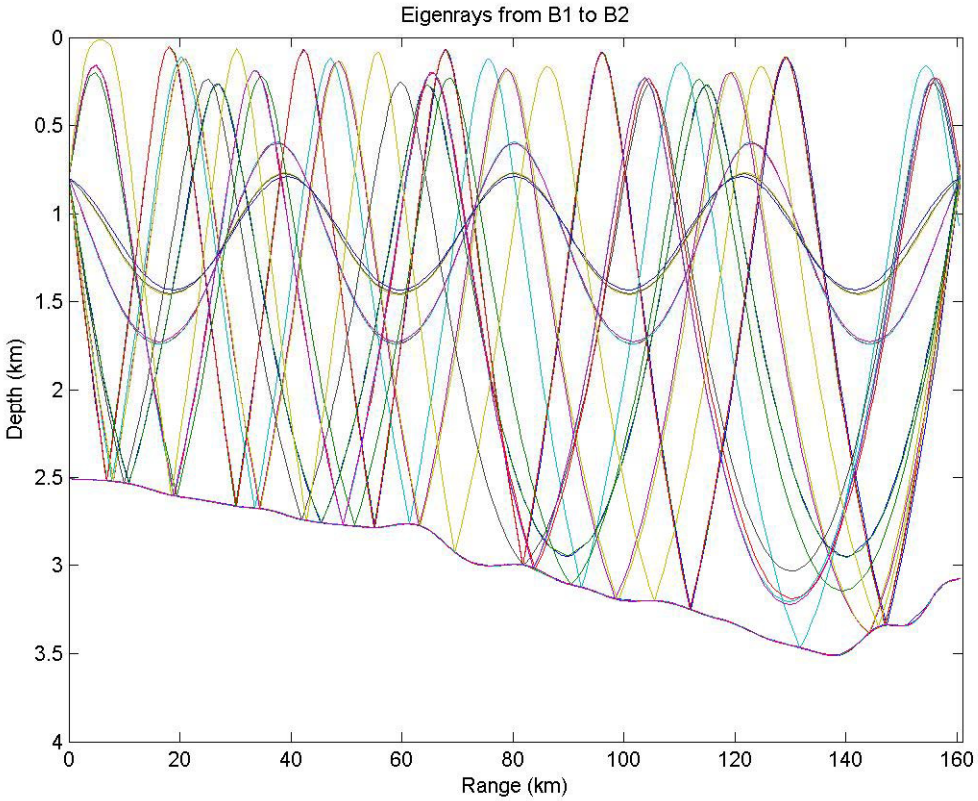

Figure 4. Modeled eigenray geometry.

C. MODELED ARRIVAL STRUCTURE

HARPO output includes eigenray geometry and travel time. A program called "ray2db" developed by Chiu (1994) was used to interpolate eigenrays and the eigenray parameters based on the ray fan computed by HARPO. This program searches for eigenrays, computes travel times to receiver, calculates phase shifts caused by turning points, bottom and surface interactions, and estimates signal loss due to raytube spreading, volume attenuation, surface scattering loss, and bottom loss.

Bottom sediment information is required as input to ray2db. Bottom sediment properties affect both the magnitude and phases of the ray arrivals. Two competing bottom sediment hypotheses represent a best and worst case scenario for WISE. Sediment characteristics received from C.-F. Chen (personal correspondence, 2005) indicated a sandy bottom referred to as "sand-silt-clay" in this paper. Core samples along the

transmission path provided by the National Geophysical Data Center (NGDC) indicate thick layers of mud or ooze intertwined with very thin layers of sand (1-3cm), referred to as "silty clay" in this paper. Accurate sediment properties are important as they affect both the magnitude of sound pressure and phase as rays reflect off the bottom. Table 2 lists the two sets of sediment characteristics used in ray2db (Medwin and Clay, 1977). The two modeled arrival patterns, including a 33 dB processing gain through pulse compression and coherent averaging, are shown in Figure 5 (a) and (b). Sand-silt-clay is considered the best case since it results in stronger arrived signals and a larger amount of detectable arrivals, ten in total (Figure 5 (a)). Silty clay is a "lossy" bottom as clearly depicted in Figure 5 (b). This bottom type is considered the worst case scenario since it results in weaker arrived signals and a smaller amount of detectable arrivals, seven in total (Figure 5 (b)). This weaker signal is associated with the increased bottom loss and decreased SNR in eigenrays with more interaction with the bottom rendering them undetectable at the receiver. If our assumptions are valid, the outcome will likely fall somewhere between these two scenarios. The intensity of the received arrivals will determine what type of bottom sediment exists on the deep basin.

Table 2. Bottom sediment characteristics inputs to ray2db.

Sediment Type	Sand-Silt-Clay Best Case	Silty Clay Worst Case
Sound Speed (m/s)	1600	1521
Density (kg/km^3)	1.7	1.24
Attenuation (dB/km/Hz)	.313	.486
Critical Angle (^{o})	19.3	6.9

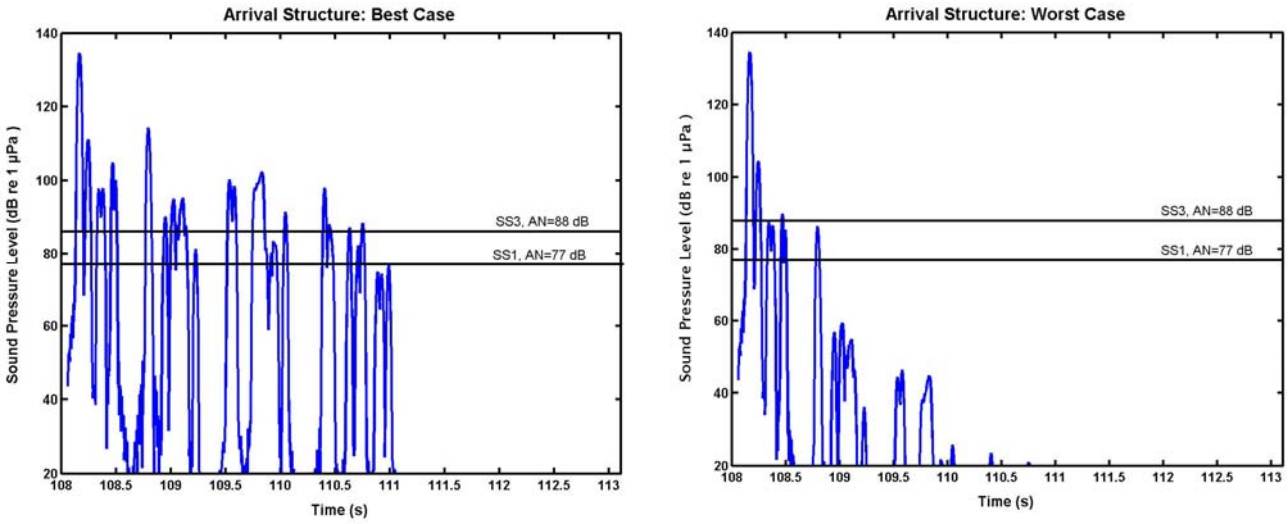

Figure 5. (a) and (b). Modeled arrival structure of best case scenario assuming sand-silt-clay bottom (a) and worst case sceario assuming silty clay bottom (b). Ambient noise lines for sea state one and three are superimposed displaying expectant SNR. Processing gain of 33 dB was added to signal.

D. RAY ARRIVALS

Model results indicate that expected received arrivals will consist of both individual eigenrays and groups of eigenrays. A group represents a set of micro-multi-path arrivals that appear at the receiver nearly simultaneously and sample nearly identical ocean space. Treating these micro-multi-path eigenrays as a single arrival modified the initial eigenray arrival pattern seen in Figure 4. Establishing a relationship between individual eigenrays through launch angle and arrival time allowed this to be accomplished. Table 3 displays these characteristics correlated to reduce the micro-multi-path signal to one unique eigenray representing the group. The individual eigenrays are color coded to indicate which are grouped. In order to be grouped together, eigenrays had to have travel time difference less than .54 seconds, launch angle difference less than .03 seconds, and follow similar ray paths (to include same number of turning points and bottom bounces). Figure 6 depicts the resulting ten predicted eigenray's arrival pattern. The final ten eigenray characteristics and geometries are seen in Table 4 and Figure 6, respectively.

As previously discussed, silty clay is a "lossy" bottom. The more an eigenray hits the bottom, the greater the bottom loss. In a silty clay environment, each bottom interaction results in greater signal loss. This is partly due to the greater absorption,

hence higher attenuation associated with this type of bottom. Bottom loss associated with a silty clay sediment range from 10-30 dB per bounce. The more bottom bounces associated with an eigenray, the weaker the received acoustic signal. Due to the multiple interactions with the bottom and the poor SNR of eigenray arrivals 8-10 shaded green in Table 4, they will not be considered reliable for the worst case scenario. When evaluating the worst case scenario, expected usable arrivals are 1-7 in Table 4. For the best case scenario, a sand-silt-clay bottom, expected usable arrivals are 1-10 in Table 4.

Table 3. Eigenray travel time and launch angle.

Eigenray	Travel Time	Launch Angle
1	109.5750	-14.8827
2	109.5579	-14.8665
3	109.5519	-14.8534
4	108.9433	-13.3214
5	108.8039	-13.0520
6	108.7888	-12.8813
7	108.3386	-10.9880
8	108.2435	-10.4270
9	108.2336	-10.4096
10	108.1580	-4.1265
11	108.1558	-4.1185
12	108.1560	-4.0262
13	108.1635	-1.3497
14	108.1639	-1.2437
15	108.1637	-0.8109
16	108.3759	11.3403
17	108.4821	12.0149
18	108.4742	12.0347
19	108.4707	12.0381
20	109.0230	14.9651

Table 4. Final ten eigenray characteristics.

Eigenray	Path	Upper Turning Point (m)	Total Turning Points	Total Bottom Bounce	Travel Time	Launch Angle	SNR
1	RR	590	7	0	108.1566	-4.09	46.5
2	RR	800	7	0	108.1637	-1.13	46.5
3	RBR	270	5	2	108.2385	-10.41	16.5
4	RBR	245	5	3	108.3386	-10.99	0
5	RBR	220	5	3	108.3759	11.34	-2
6	RBR	200	6	3	108.4757	12.03	-3
7	RBR	160	4	5	108.7964	-12.97	-4
8	RBR	130	5	5	108.9430	-13.32	-32
9	RBR	100	5	5	109.0230	14.97	-29
10	RBR	100	5	6	109.5750	-14.87	-41.5

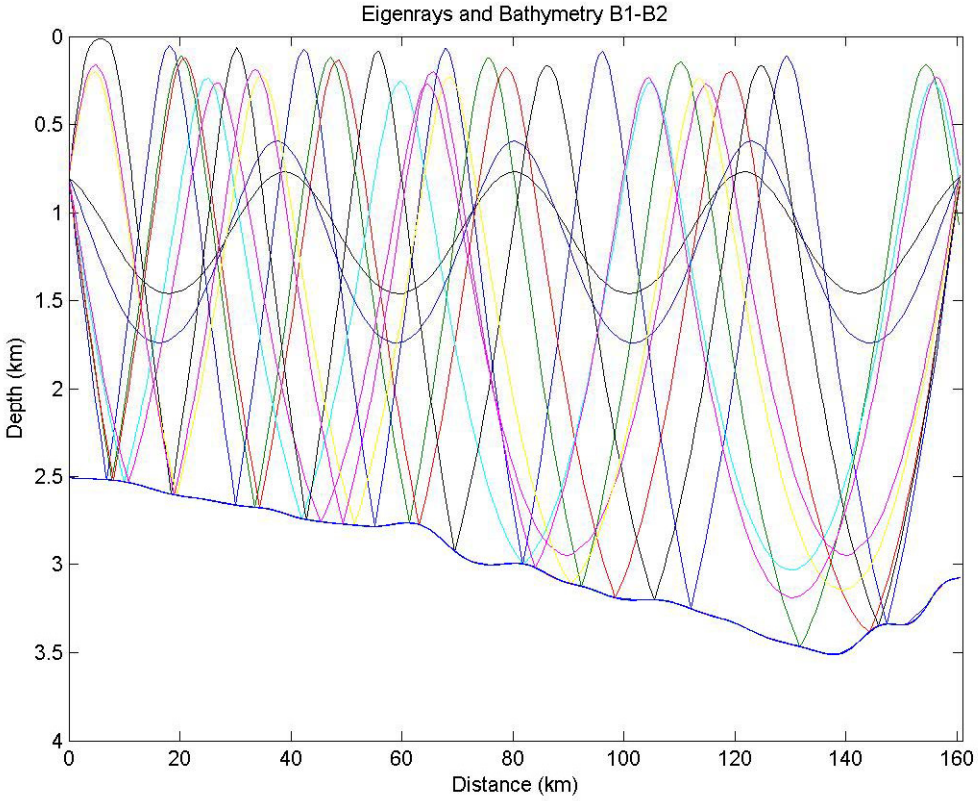

Figure 6. Final ten eigenray paths.

E. SIGNALING SCHEME

Figure 5 (b), demonstrates our expectant SNR for a silty clay bottom. This is our worst case scenario, and if this represents reality well, it clearly demonstrates the need for alternative signaling schemes and/or additional processing gain in order to attain multiple reliable acoustic signals at the receiver. A traditional approach to underwater acoustic signal design and processing is described by Birdsall and Metzger, 1986. This method uses phase modulation and periodic signals to eliminate self-clutter. These signals are generated using digital techniques by exploiting phase modulation of the periodic signals using maximal length binary sequences (m-sequences) to achieve multiple pulse compression with no side lobes. Modulating the phase with an m-sequence and applying a correlation-matched filter while signal processing results in a finite, narrow pulse. This modulation allows an increase in signal duration, allowing adequate SNR at long range to perform the resolution of individual ray arrivals. This leads to processing gain already discussed and displayed in Table 1. This gain is based on the characteristics of the WISE deep mooring transducer seen in Table 5.

In order to resolve eigenrays 1 through 7 in the mean ocean of sea state 3, a minimum SNR goal of 10 dB is desired. To achieve this, additional processing gains of at least 14 dB, resulting in a total processing gain of 47 dB, is needed. This can be accomplished through additional pulse compression by increasing the number of transmission sequences, thus improving SNR.

Coherent averaging of m-sequence cycles may improve the SNR by 10 log (N), where N is the number of cycles during a separate reception. Varying N from 10 to 100 yields improvement from 10 dB to 20 dB, respectively. Add that to the 27 dB already gained from pulse compression results in processing gains of 37 dB to 47 dB. Based on the modeled travel time estimates, acoustic propagation will take approximately 108-109 seconds. The proposed transmission times, shown in Table 5, were based on a several hardware constraints. Each transceiver must collect, process, and store the other source's transmission, monitor its own systems, and establish a stable phase-locked loop prior to system operations adding time requirements to receiver operations.

Additionally, a 10-minute period sampling rate is needed to ensure sufficient temporal resolution exists to capture acoustic variability caused by internal waves as they

transit the basin. Although short-period (10-minute) internal waves have been directly measured by isotherm motion measured by sensors on the southern China continental shelf (Duda, et al., 2004), there have been none measured as they propogate across the basin. Huge internal solitons observed by SAR images indicate wavelengths of 500 m-5000 m with wave speeds up to 1.9 m/s (Hsu, Liu, 2000). This would indicate periods of 5-45 minutes. The internal tidal period is known to be either semi-diurnal or diurnal, thus having approximately a scale of 12 or 24 hours. A 10-minute period sampling rate is more than adequate to sample the internal tide and quantify the acoustic variability caused by internal waves.

Increasing the number of sequences to N=100 provides a coherent averaging gain of 20 dB. This allows for adequate SNR to resolve all seven eigenrays in the worst case scenario, but results in an undesirable sampling rate. This would likely permit the resolution of all seven eigenrays, however, may not provide sufficient temporal resolution to measure acoustic variability.

If the worst case bottom hypothesis proves to be correct, some post experimental remedies will be required to increase gain. Under these circumstances, additional coherent averaging is recommended to draw the received signal out of the noise.

Table 5. WISE deep basin transmission source characteristics.

Start Time (UTC)	
Transmission Times (minutes after hour)	0, 10, 20, 30, 40, 50
Center Frequency	400
Bandwith	100
Source Level	180 dB re 1 μPa @ 1m
Cycles Per Digit	4
Digit Width	10 ms
Digits per sequence (sequence length)	511 (5.11 s)
Number of sequences transmitted (length of transmission)	5 (25.55 s)
m-sequence LAW (octal)	1533
Sequence initialization	000000001
Phase modulation angle	87.46035^{o}
Number of sequences received and averaged	4

THIS PAGE INTENTIONALLY LEFT BLANK

III. INVERSE METHOD

A. VERTICAL STRUCTURE

The approach used to study the inverse problem is a stochastic inverse method. Details on this method can be found in Chiu et al, 1994. This method gives resolution approximations and solution error, aiding in the oceanographic interpretation. Dynamical mode analysis is the method used for analyzing the vertical structure to constrain the tomographic estimate. This is a common statistical method for analyzing oceanographic variability across spatial scales.

The vertical structure of the oceanic fluctuations in the model area is primarily composed of a few lower vertical modes (Chiu, et al., 1987). To this point, almost all internal waves observed in nature are mode-1 depression waves (Liu, et al., 1998). Duda et al. (2004) also noted that nonlinear internal waves at the northern South China Sea continental slope were well approximated by mode-1 solutions in the vertical. For the same region, Ramp, et al. (2004) observed solitons characteristic of classic mode-1 waves. Chiu, et al. (2004) used results from vertical decompositions, to show modal analysis was representative of the cross-shelf, sound speed perturbations in the South China Sea. Additionally, only two modes were needed to capture 77-95% of the variances. The first mode consistently accounted for 70% of the variance. Based on these studies, mode one is concluded to be the dominant mode. However, because these results are based in much shallower water, analysis of mode-2 was done to determine the resolution and likelihood of observing the internal tide if mode-2 is present. Figure 7 shows the first two dynamical vertical modes of sound speed perturbation. These modes were normalized to have unit energy.

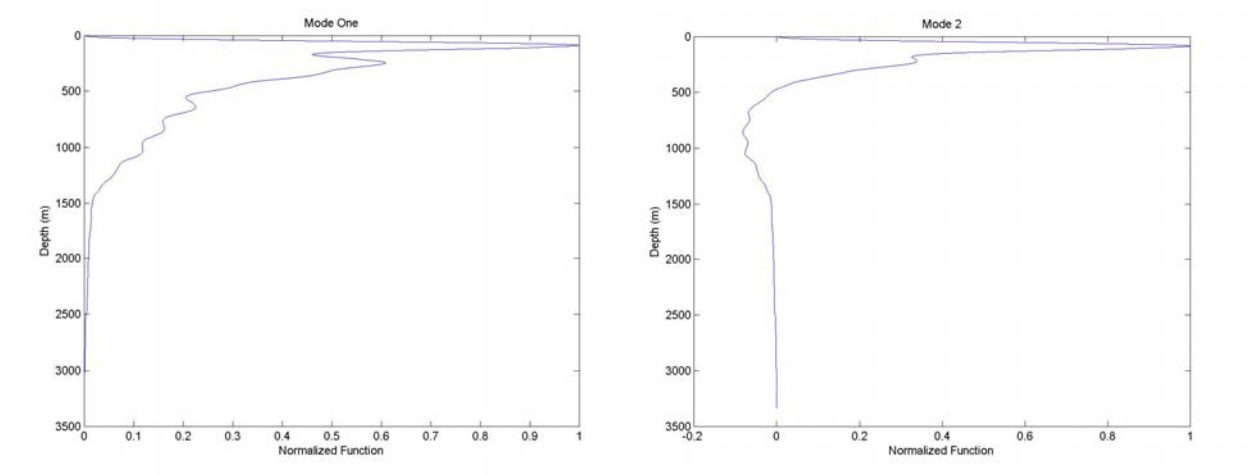

Figure 7. Normalized vertical sound speed perturbation modes 1 and 2.

B. INTERNAL TIDE WAVELENGTH

The internal tide wavelength across the South China Sea deep basin has not been measured and remains unknown. This is just one mystery WISE is seeking to answer. The dominant tides of this region are mixed with both diurnal and semi-diurnal components. On the northern South China Sea continental slope, Duda, et al., 2004, observed wavelengths of semidiurnal internal tides on a 30 km scale, diurnal internal tides on a 100 km scale, and internal waves from 46-90 km. During ASIAEX-2001, deployed moorings were able to make in-situ observations of internal waves. SAR imagery was also used to observe these waves. Estimated observed wavelengths for in-situ measurements and imagery varied. Moorings estimates ranged from 4.8-13.6 km (Ramp, et al., 2004) while SAR imagery estimates ranged from 14-26 km (Liu et al., 2004). These comparisons demonstrate the complexity of using surface information to infer the in-situ properties of waves as SAR imagery brightness depends on the variety of air/sea interaction and strongest image reflections may not be the same as the strongest in-situ signals (Ramp, et al., 2004). They also demonstrate the need for additional remote monitoring techniques like tomography to aid in understanding internal tide progression and the phenomenon associated with it. Mapping the internal tide will provide insight into other remaining scientific questions of internal wave activity in the deep basin.

C. INVERSE SOLUTION AND TOMOGRAPHIC RESOLUTION

If sound speed along the eigenray varies as a function of range, depth and time, then this variation can be described by a linear composition of n modes:

$$\delta c(x,z,t)= \sum_{i=1}^{n} a_i(x,t) f_i(z)$$

where $a_i(x,t)$ is the time and range varying amplitude of the mode and $f_i(z)$ is the i^{th} dynamical mode for internal tides. Because the wavelength of the internal tide is unknown, a sensitivity analysis was conducted using several iterations of the inversion. The hypothesized internal tide wavelength is 30-100 km; hence, decorrelation lengths were varied from 20-100 km to gain an appreciation of expectant internal tidal resolution and understand its associated variance. Additionally, the vertical structure was constrained by mode-1, then again by the first two sound speed perturbation modes. Inversions were done for both the best case scenario, resolving ten eigenrays with a sand-silt-clay bottom, and worst case scenario, resolving only seven eigenrays with a silty clay bottom.

Horizontal resolution lengths of the tomographic estimate for the best and worst case scenarios (decorrelation length of 30 km) are illustrated in Figure 8. This represents the smallest ocean feature that can be observed along the transmission path. The best case scenario results in minimum resolution length of 25-50 km for ranges of 20-160 km. Worst case results in 30-60 km for the same range scale. For mode-2, Figure 9, minimum resolution lengths of 80-100 km can be expected, for both best and worst case. If mode-2 is present, mode-1 will see a decrease in resolution by at least 20 km. Locations near the transmitter have poor resolution due to the minimal density of raypath crossings, while the location near the receiver has the greatest resolution due to the maximum density of raypath crossings here.

The uncertainty estimate or mean square error in percentage is illustrated in Figures 10 for mode-1 and Figure 11 for mode-2. Mode-1 has an estimated mean square error of less than 30% for the best case and 10-50% for the worst. Analysis of mode-2 reveals error of greater than 60% for both scenarios. Mode-1 error also increases in the presence of mode-2.

A sensitivity analysis was done by running several iterations of the inversion with varying decorrelation lengths. The results of this sensitivity analysis are displayed in Table 6. Based on this table, it is clear that the internal tide will be resolved accurately if wavelengths are 30-100 km in length.

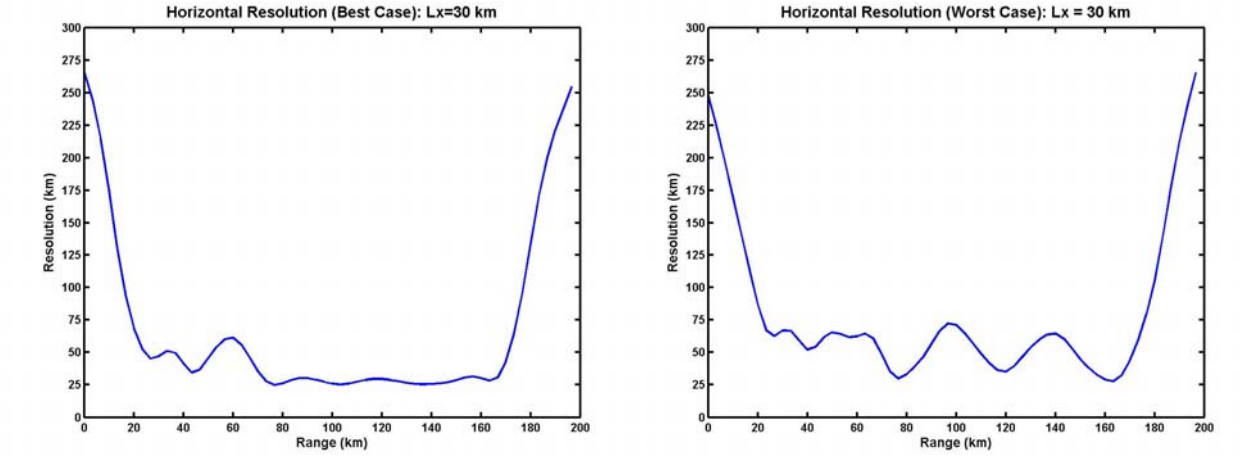

Figure 8. (a) and (b). Horizontal resolution of the tomographic estimate for mode-1, decorrelation length of 30 km: best case scenario (a) worst case scenario (b).

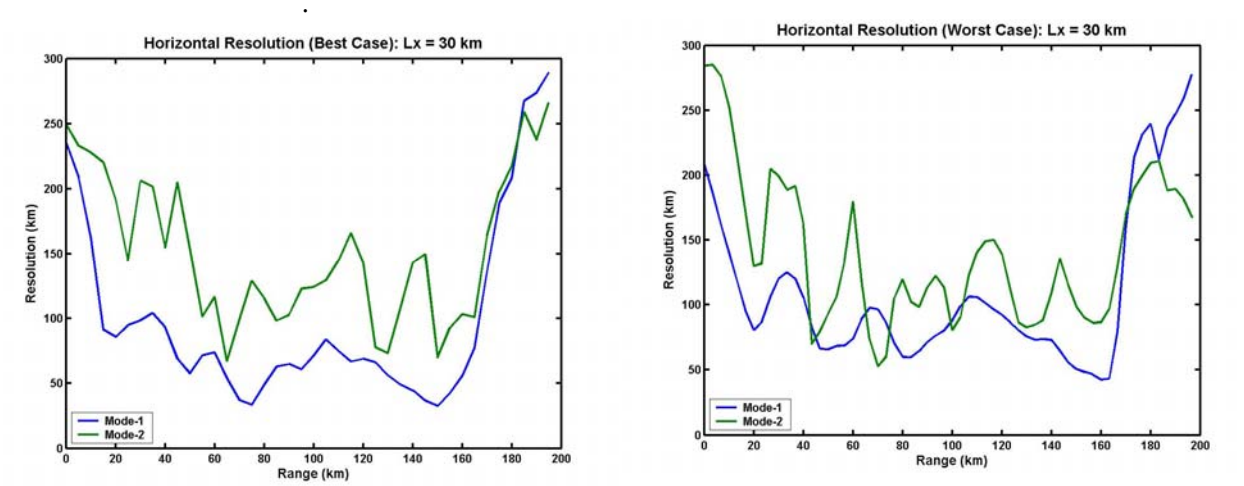

Figure 9. (a) and (b). Horizontal resolution of the tomographic estimate for mode 1 and 2, decorrelation length of 30 km: best case scenario (a) worst case scenario (b).

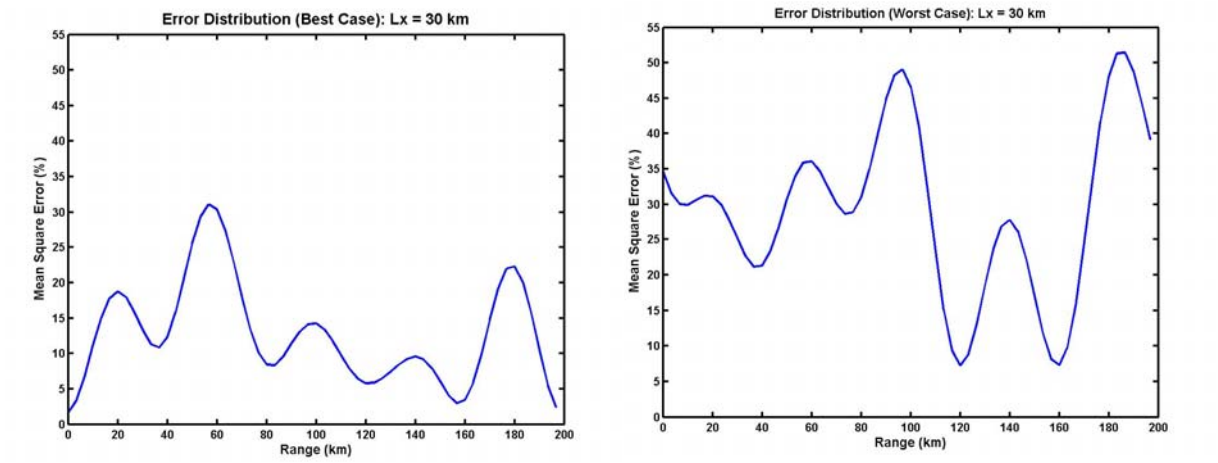

Figure 10. (a) and (b). Mean square error tomographic estimate for mode-1, decorrelation length of 30 km: best case scenario (a) worst case scenario (b).

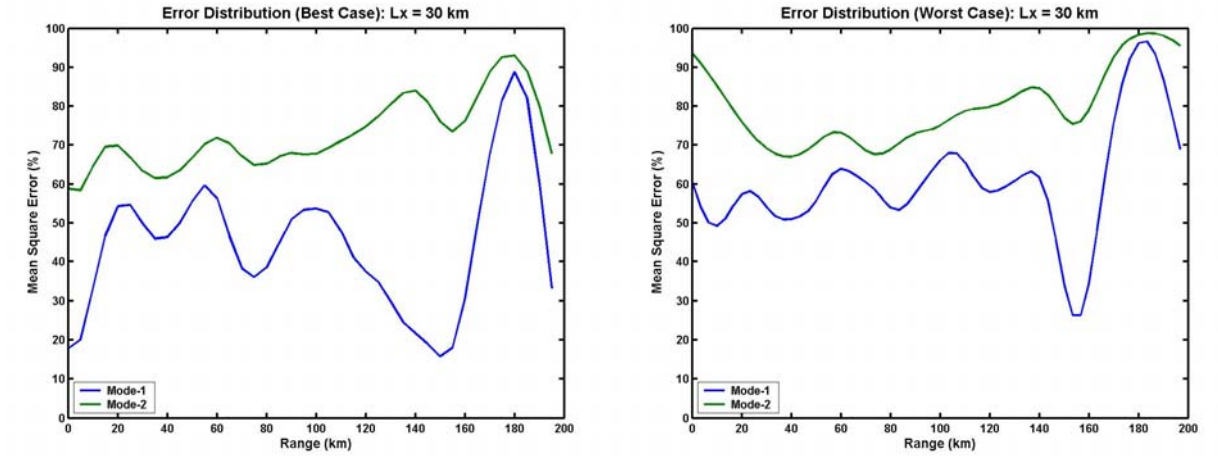

Figure 11. (a) and (b). Mean square error tomographic estimate for mode 1 and 2, decorrelation length of 30 km: best case scenario (a) worst case scenario (b).

Table 6. Sensitivity analysis for best and worst case scenarios.

Best Case		
Decorrelation Length (km)	Minimum Resolution (km)	Mean square error (%)
20	21.6	33.1
30	25.5	12.7
40	29.9	5.3
50	36.4	2.8
60	44.5	1.8
100	75.4	.0.3

Worst Case		
Decorrelation Length (km)	Minimum Resolution (km)	Mean square error (%)
20	41.6	50.0
30	29.5	29.2
40	32.6	14.3
50	38.7	7.5
60	47.2	4.1
100	76.7	0.8

IV. CONCLUSIONS

The objective of this thesis was to determine whether detectable and resolvable arrivals would occur during WISE. An additional objective was to determine the likelihood of monitoring the progression of internal tides as they transit the South China Sea deep basin. This analysis involved propagation modeling and a tomographic inverse method. The ray-theory approach was used to model the arrival structure with a reference ocean. These model results indicate detectable, resolvable arrivals are to be expected. The number and strength of these arrivals depends greatly on the environment, specifically the bottom characteristics. Competing bottom characteristic hypotheses were tested leading to a best and worst case scenario. If post experiment processing indicates the worst case scenario is more representative of reality, additional coherent averaging will needed to ensure the best tomographic resolution.

A linear inversion was conducted with the solution's vertical structure constrained by dynamical sound speed perturbation modes. This resulted in an estimate of the horizontal resolution and variance. Mode-1 will likely be the dominant factor in internal tides transiting the deep basin, and the majority of analysis was based on this assumption. However, this assumption was based on shallow water studies, so mode-2 was evaluated as well. This was to investigate whether the internal tide will be resolved if mode-2 is present. If mode-2 is indeed present, this experiment is not expected to resolve the internal tide sufficiently.

If mode-1 assumption is valid, WISE deep basin experiment should successfully monitor the progression of the internal tide. It is assumed the diurnal internal tide wavelength is on the order 100 km and semi-diurnal 30 km. A sensitivity analysis varying the decorrelation length and using both best and worst case scenarios indicates tomography is expected to reveal the internal tide with an error less than 30%. Bottom sediment samples will be taken during the experiment as well. If it is discovered that the basin contains more of sandy sediment, it is possible the monitoring results will be better than projected in this paper. Additionally, results are expected to be better for decreased sea state, but are also expected to be worse for stormy periods.

THIS PAGE INTENTIONALLY LEFT BLANK

LIST OF REFERENCES

Birdsall, T.G., Metzger, K. J., "Factor Inverse Matched Filtering," *Journal of the Acoustic Society of America*, 79(1), 1986.

Chen, C.-F., Personal Correspondance, 2004.

Chiu, C.-S., "Naval Postgraduate School Proposal for Research," 2004.

Chiu, C.-S., Desaubies, Y., "A Planetary Wave Analysis Using the Acoustic and Conventional Arrays in the 1981 Ocean Tomography Experiment," *Journal of Physical Oceanography*, 17, pp 1270-1287, 1987.

Chiu, C.-S., Miller, J. H., Lynch, J. F., "Forward Coupled-Mode Propagation Modeling for Coastal Acoustic Tomography," *Journal of the Acoustic Society of America*. 99(2), 1996.

Chiu, C.-S., Ramp, S. R., Miller, S.W., Lynch, J. F.,. Duda, T.G, Tang, T.-Y, Acoustic intensity fluctuations induced by South China Sea internal tides and solitons," *IEEE J. Oceanic Engineering*, 29, 2004.

Chiu, C.-S., Semtner, A.J.,Ort, C.M., Miller, J.H., Ehert, L.L, "A Ray Variability Analysis of Sound Transmissions from Heard Island to California," *The Journal of the Acoustic Society of America*, Vol. 96(4), pp 2380-2388, 1994.

Clark, V., "Sea Power 21," *Proceedings*, October, 2002.

Duda, T.F., Lynch, J. F., Irish, J.D., Beardsley, R.C., Ramp, S.R., Chiu, C.-S., Tang, T. Y., Yang, Y.-J., "Internal Tide and Nonlinear Internal Wave Behavior at the Continental Slope in the Northern South China Sea," *IEEE J. Oceanic Engineering*, 29, 2004.

Hsu, M.-K., Liu, A.K., and Liu, C., "Nonlinear internal waves in the South China Sea," *Canadian J. Remote Sensing*, 26, 72-81, 2000.

Hull, R.E., "The South China Sea: Future Source of Prosperity or Conflict in South East Asia?" Strategic Forum, 60, 1996.

Jones, R.M., Riley, J.P., Georges, T.M., "HARPO: A Versatile Three-Dimensional Hamiltonian Ray Tracing Program for Acoustic Waves in Ocean with Irregular Bottom," Wave Propagation Laboratory, National Ocean and Atmospheric Administration, Boulder, CO, 457 pp., 1986.

Liu, A. K., Y. S. Chang, M.-K. Hsu, and N. K. Liang, "Evolution of nonlinear internal waves in the East and South China Seas," *Journal of Geophysical Research*. 103, 7995-8008, 1998.

Liu, A.K., Zhao, Y., Yang T.Y., Ramp, S. R, "Model-Data Assimilation of Internal Waves During ASIAEX-2001," *IEEE J. Oceanic Engineering*, 2004.

Medwin, H., Clay, C.S., "Fundamentals of Acoustical Oceanography," Academic Press. San Diego, CA 1998.

Morvillez, T., "Monitoring Temperature Variability Along the California Coast Using Acoustic Tomography," Master's Thesis, Naval Postgraduate School – Monterey, CA, September 1997.

Munk, W., Worcester, P., Wunsch, C., "Ocean Acoustic Tomography," Cambridge University Press, New York, 1995.

Neander, D.O., "Analysis of Temperature Variability Between Davidson Seamount and Sur Ridge: The Tomographic Inverse Problem," Master's Thesis, Naval Postgraduate School – Monterey, CA. June 2002.

Ramp, S.R.,Yang, T.-Y., Duda, T.F., Lynch, J.F., Liu, A.K., Chiu, C.-S., Bahr, F., Kim, H.-R., Yang, Y. J., "Internal solitons in the northeastern South China Sea Part I: Sources and deep water propogation," *IEEE J. Oceanic Engineering*, 29, 2004.

INITIAL DISTRIBUTION LIST

1. Defense Technical Information Center
   Ft. Belvoir, VA

2. Dudley Knox Library
   Naval Postgraduate School
   Monterey, CA

3. James Lynch
   Woods Hole Oceanographic Institution
   Woods Hole, MA

4. Steve Ramp
   Naval Postgraduate School
   Monterey, CA

5. Ellen Livingston
   Office of Naval Research
   Arlington, VA

6. Ching-Sang Chiu
   Naval Postgraduate School
   Monterey, CA

7. Chris Miller
   Naval Postgraduate School
   Monterey, CA

8. Adria Schneck-Scott
   Office of Naval Intelligence
   Washington, DC